

May 20, 2010

## Magnetotransport properties of Mn-Si-C based nanostructures

Sungmu Kang  
*Catholic University of America*

Greg A. Brewer  
*Catholic University of America*

Battogtokh Jugdersuren  
*Catholic University of America*

Robert DiPietro  
*Northeastern University*

Don Heiman  
*Northeastern University*

*See next page for additional authors*

---

### Recommended Citation

Kang, Sungmu; Brewer, Greg A.; Jugdersuren, Battogtokh; DiPietro, Robert; Heiman, Don; Buechele, Andrew C.; McKeown, David A.; Pegg, Ian L.; and Philip, John, "Magnetotransport properties of Mn-Si-C based nanostructures" (2010). *Physics Faculty Publications*. Paper 178. <http://hdl.handle.net/2047/d20001189>

---

**Author(s)**

Sungmu Kang, Greg A. Brewer, Battogtokh Jugdersuren, Robert DiPietro, Don Heiman, Andrew C. Buechele, David A. McKeown, Ian L. Pegg, and John Philip

## Magnetotransport properties of Mn–Si–C based nanostructures

Sungmu Kang,<sup>1</sup> Greg A. Brewer,<sup>2</sup> Battogtokh Jugdersuren,<sup>1,3</sup> Robert DiPietro,<sup>4</sup> Don Heiman,<sup>4</sup> Andrew C. Buechele,<sup>1</sup> David A. McKeown,<sup>1</sup> Ian L. Pegg,<sup>1,3</sup> and John Philip<sup>1,3,a)</sup>

<sup>1</sup>The Vitreous State Laboratory, The Catholic University of America, Washington DC 20064, USA

<sup>2</sup>Department of Chemistry, The Catholic University of America, Washington DC 20064, USA

<sup>3</sup>Department of Physics, The Catholic University of America, Washington DC 20064, USA

<sup>4</sup>Department of Physics, Northeastern University, Boston, Massachusetts 02115, USA

(Received 1 March 2010; accepted 31 March 2010; published online 20 May 2010)

Boron-incorporated Mn<sub>5</sub>SiC nanowires were grown using chemical vapor deposition method. The nanowire cluster exhibits magnetic hysteresis loops at room temperature and the strength of the magnetic behavior depends on the concentration of the boron incorporation. Mn<sub>5</sub>SiC nanowire-based devices exhibit spin dependent transport properties which shows significant changes with boron content. Large magnetoresistance is observed in lightly boron-incorporated nanowire devices and it decreases with increase in boron content. © 2010 American Institute of Physics. [doi:10.1063/1.3425780]

MnSi is a well-known weak itinerant helimagnet with a magnetic phase transition occurring around 29.0 K at ambient pressure.<sup>1–7</sup> Application of external magnetic fields results in field-induced phase transitions from the helimagnetic phase to a conical spin structure at low fields and then to a ferromagnetic state at higher magnetic fields.<sup>1</sup> The temperature dependence of high field magnetization of field-induced ferromagnetic states of MnSi shows signatures indicating the role of both spin wave excitations and stoner band excitations related to itinerant electron ferromagnetism.<sup>8</sup> Recently, there are reports citing that incorporating carbon to Mn–Si system results in compounds that exhibit magnetic ordering near or well above room temperature.<sup>9–11</sup> We have reported the feasibility of growing Mn<sub>5</sub>SiC nanostructures using an organometallic Mn precursor.<sup>12</sup> In this communication, we report the magnetotransport properties of these nanostructures by growing them from differently boron-doped silicon substrates.

The growth of Mn<sub>5</sub>SiC nanowires were carried out using chemical vapor deposition involving a coordination complex precursor for Mn and C, which has been already reported elsewhere.<sup>12</sup> The silicon substrate is used as the source for silicon in Mn<sub>5</sub>SiC nanostructures. We have used silicon substrates with three different boron doping for the growth of these nanowires. The boron doping concentrations were  $2 \times 10^{17}/\text{cm}^3$ ,  $5 \times 10^{18}/\text{cm}^3$ , and  $5 \times 10^{19}/\text{cm}^3$ , respectively. The nanowires grown from these substrates will be referred to as low, medium, and heavy-boron-incorporated nanowires (LBNW, MBNW, and HBNW), respectively, in this article. Highly dense boron-incorporated Mn<sub>5</sub>SiC nanowires were grown as shown in Fig. 1 (inset). Nanowire size ranges from 50–100 nm. Figure 1 illustrates the x-ray diffraction pattern of nanowires grown from three different silicon substrates. All of the grown nanowires exhibit orthorhombic structure with Cmc21 space group. The lattice parameters for the grown nanowires are  $a=10.198 \text{ \AA}$ ,  $b=8.035 \text{ \AA}$ , and  $c$

$=7.630 \text{ \AA}$ , respectively. There is no systematic shift of the peaks with boron incorporation to elucidate whether there is a lattice volume change. It would be possible that the varying size range (50–100 nm) and the stress in the nanowires on different sets also contribute to the line width and broadening.<sup>13</sup> Gold nanoparticles (100 nm) were used as catalyst for the nanowire growth, thus, in addition to the formation of Mn<sub>5</sub>SiC nanowires, formation of a small fraction of Au<sub>5</sub>Si<sub>2</sub> particles was also observed. The peaks corresponding to the Au<sub>5</sub>Si<sub>2</sub> phase are marked in Fig. 1. High-resolution transmission electron microscopy (HRTEM) studies of these nanowires support the x-ray diffraction results and the detailed HRTEM studies on Mn<sub>5</sub>SiC nanowires are reported in our earlier publication.<sup>12</sup> In order to understand whether the boron actually goes into the nanowire, we have carried out secondary ion mass spectroscopy studies (SIMS). A cleaning procedure was carried out to make sure that the surface of the nanowires is clean of any residues. In this process, the as-grown nanowires were etched for a short time in 5% HF solution. Then, the nanowires from the as-

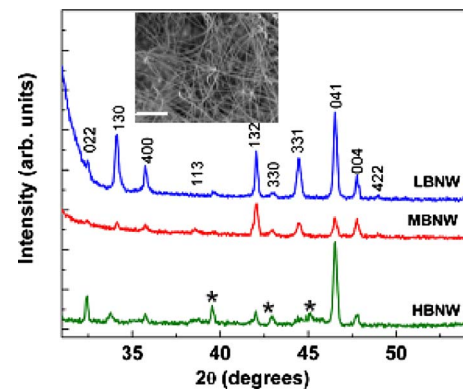


FIG. 1. (Color online) X-ray diffraction patterns of boron-incorporated nanowires grown from different silicon substrates (a) LBNW, (b) MBNW, and (c) HBNW. The peaks corresponding to Au<sub>5</sub>Si<sub>2</sub> phase are marked. The inset shows the scanning electron microscopy image of boron-incorporated Mn<sub>5</sub>SiC nanowires. The scale bar corresponds to 1  $\mu\text{m}$ .

a)Electronic mail: philip@cua.edu.

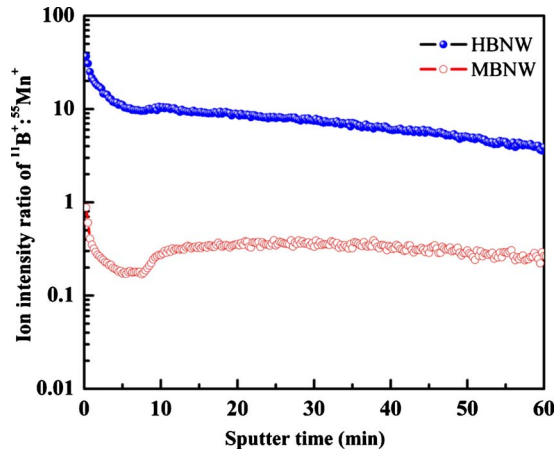
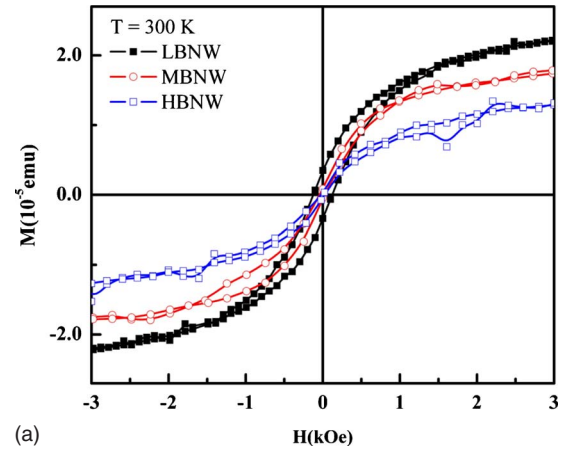


FIG. 2. (Color online) SIMS data for MBNW and HBNW nanowires.

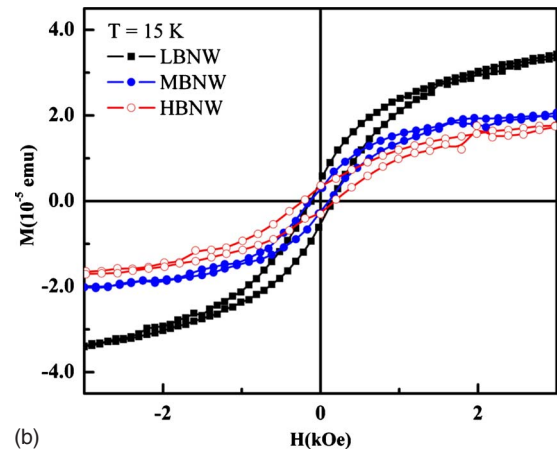
grown substrates are removed using sonication and are transferred to an undoped silicon substrate for SIMS analysis. SIMS sputter profiling analysis was performed using a 100 nA, 17 keV,  $^{16}\text{O}^-$  primary beam with a square raster of  $250\ \mu\text{m}$ . Figure 2 displays the SIMS data for medium and heavy-boron-incorporated nanowires. The plots clearly indicate that the boron-intensity from HBNW's is strong, compared to the other. The plots show two characteristic regions, an initial transient region with a sudden change in the signal intensity, where the nanowires are modified by oxygen incorporation and build-up due to the  $\text{O}^-$  primary ion beam bombardment. After about 9 or 10 min of sputtering time, starting with a characteristic bump, data exhibits a steady-state region, where the nanowires are in oxidation equilibrium. The intensities of the signals from the two nanowire sets differ by a factor of 18 and there is slight variation in this factor as the sputter time increases. The boron concentration in the two Si substrates used for growing these nanowires differs by a factor of 25. This confirms the presence of boron in the nanowires and the signal that is detected purely arises from the highly dispersed nanowire cluster on the undoped Si substrate. A quantitative estimate of boron content in each of these sets was difficult because of the unavailability of a boron standard for this particular measurement.

The magnetic hysteresis loops were measured using a superconducting quantum interference device magnetometer. The data for three different samples at 300 and 15 K are displayed in Fig. 3. The external magnetic field is applied parallel to the substrate plane. The nanowire ensembles exhibit clear magnetic hysteresis at these two temperatures. The coercive fields are 120 Oe, 45 Oe, and 26 Oe, respectively, at room temperature with the increase in doping concentration. Hysteresis loops show a decreasing trend in saturation and remanence magnetizations with increase in boron content in the nanowires. Although, a direct comparison of all three samples can be made only after normalizing the data, but normalization is difficult because of the complication in calculating the mass or volume of the nanowire ensembles.

Nanowire devices are fabricated with standard electron beam lithography for magnetotransport measurements.<sup>12</sup> The scanning electron microscopy image of a typical device with



(a)



(b)

FIG. 3. (Color online) The magnetic hysteresis loops of the three sets of nanowires at (a) 300 and (b) 15 K. The magnetic field is applied parallel to the substrate plane.

the magnetotransport measurement configuration is displayed in the inset of Fig. 4(a). The electrodes on the nanowire channels are layers of Al(100 nm)/Au (5 nm) evaporated using an ultrahigh vacuum thin film deposition system. The current-voltage ( $I$ - $V$ ) measurements were carried out using a semiconductor parametric analyzer (Agilent 4156 C). Both LBNW and HBNW nanowire devices show nonlinear  $I$ - $V$  characteristics with currents in the range of nanoamperes [Figs. 4(a) and 4(b)]. In the presence of small external magnetic fields applied along the axial direction of the nanowires ( $H=300$ – $1000$  Oe), there is a large change in the  $I$ - $V$  characteristics in the case of a device fabricated with LBNW's. The change is almost a factor of 4 at higher bias voltages, but there is an insignificant change in the case of devices with HBNW's. The magnetoresistance (MR) is calculated using the expression,  $\{100\%[(R_{B=0\text{ Oe}} - R_{B=700\text{ Oe}})/R_{B=0\text{ Oe}}]\}$ . The MR value is as high as  $\sim 80\%$  at room temperature for the low-boron-doped nanowire device and it is nearly negligible for the HBNW device. Comparing the magnetization, and magnetotransport properties of the nanowires and their devices, nanowires that display strong magnetic behavior exhibit large MR. Large incorporation of boron into the nanowires decreases the magnetic coupling and in turn considerably reduces the MR.

As discussed earlier  $\text{Mn}_5\text{SiC}$  is an orthorhombic carbide and the unit cell consists of eight formula units.<sup>14</sup> The bulk

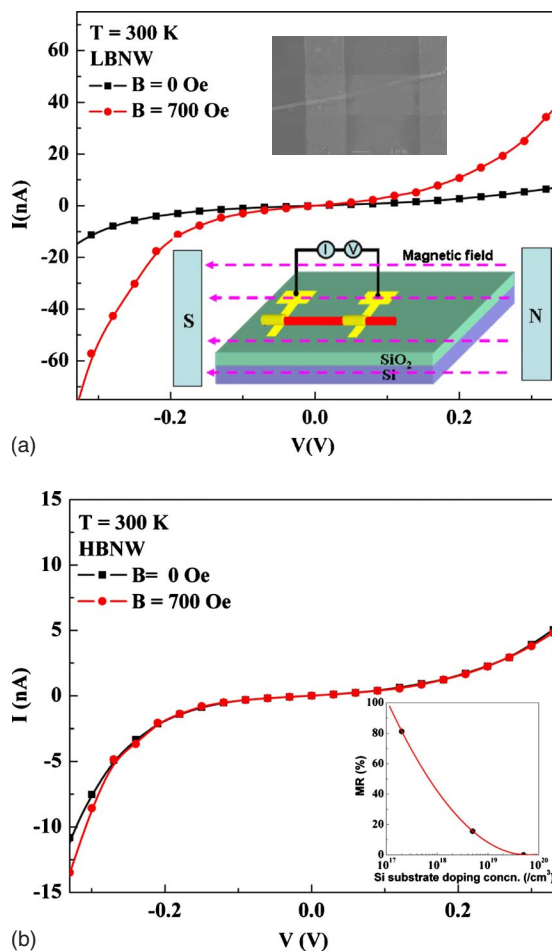


FIG. 4. (Color online) Current-voltage characteristics of (a) LBNW and (b) HBNW nanowire devices with and without the presence of external magnetic field (700 Oe). Inset in (a) shows the SEM image of a typical device and also illustrates the magnetotransport measurement configuration. Inset in (b) shows MR of the nanowire devices decreases with the incorporation of boron. The x-axis gives the boron concentration of the silicon substrates that are used for the nanowire growth.

$\text{Mn}_5\text{SiC}$  has been shown to exhibit ordered magnetic behavior with a Curie temperature around 284 K.<sup>15</sup> The neutron diffraction studies on  $\text{Mn}_5\text{SiC}$  have reported that the bulk magnetic structure is complex and can be described by both an antiferromagnetic and a helimagnetic sublattices. The  $\text{Mn}_5\text{SiC}$  nanostructures that we have grown with no boron/low-boron incorporation exhibit magnetic hysteresis even above 400 K.<sup>12</sup> Thus, the  $T_c$  of the  $\text{Mn}_5\text{SiC}$  nanostructures is much higher than that reported for the bulk. This might be possible due to the changes in the magnetic sublattices in the nanostructures. The nanostructures may have mostly helimagnetic or canted spin structure in comparison to the mixed antiferromagnetic and helimagnetic sublattices in the bulk. The stress induced enhancement of Curie temperature is also reported in several other systems.<sup>16,17</sup> The stress in one-dimensional structures can increase the magnetic exchange interaction leading to enhanced Curie temperature as it is reported for strontium or calcium doped perovskite

manganites.<sup>18,19</sup> The large spin-dependent transport properties observed in LBNW's may be arising as a result of the change in helimagnetic or canted magnetic behavior to strong ferromagnetic behavior even with small applied external magnetic fields as in the case of  $\text{MnSi}$ .<sup>1,8</sup> It is possible that the incorporation of boron into the lattice changes the local environment of the Mn ions and thereby decreasing the exchange interaction which in turn affect the magnetotransport properties. Thus, no boron or low-boron-incorporated nanostructures exhibit large magnetotransport properties but the MR decreases with increase in boron content. A systematic study of the MR of these systems as a function of temperature at high magnetic fields is under progress to elucidate the exchange mechanism.

In summary, we have shown that the magnetotransport properties of  $\text{Mn}_5\text{SiC}$  nanostructures can be considerably altered by incorporating boron. Large MR of  $\sim 80\%$  is observed at low external magnetic fields with low-boron-incorporated  $\text{Mn}_5\text{SiC}$  nanostructure devices.

## ACKNOWLEDGMENTS

This work has been supported by funding from NSF under CAREER Grant No. ECCS-0845501 and NSF-MRI under Grant No. DMR-0922997. We thank Cathy Paul for carefully reading through the manuscript.

- <sup>1</sup>Y. Ishikawa, K. Tajima, D. Bloch, and M. Roth, *Solid State Commun.* **19**, 525 (1976).
- <sup>2</sup>D. Belitz, T. R. Kirkpatrick, and T. Vojta, *Phys. Rev. Lett.* **82**, 4707 (1999).
- <sup>3</sup>C. Pfleiderer, P. Böni, T. Keller, U. K. Rößler, and A. Rosch, *Science* **316**, 1871 (2007).
- <sup>4</sup>S. M. Stishov, A. E. Petrova, S. Khasanov, G. K. Panova, A. A. Shikov, J. C. Lashley, D. Wu, and T. A. Lograsso, *Phys. Rev. B* **76**, 052405 (2007).
- <sup>5</sup>S. Kusaka, K. Yamamoto, T. Komatsubara, and Y. Ishikawa, *Solid State Commun.* **20**, 925 (1976).
- <sup>6</sup>S. Tewari, D. Belitz, and T. R. Kirkpatrick, *Phys. Rev. Lett.* **96**, 047207 (2006).
- <sup>7</sup>B. Binz, A. Vishwanath, and V. Aji, *Phys. Rev. Lett.* **96**, 207202 (2006).
- <sup>8</sup>M. K. Chattopadhyay, P. Arora, and S. B. Roy, *J. Phys.: Condens. Matter* **21**, 296003 (2009).
- <sup>9</sup>C. Sürgers, M. Gajdzik, G. Fischer, H. v. Löhneysen, E. Welter, and K. Attenkofer, *Phys. Rev. B* **68**, 174423 (2003).
- <sup>10</sup>B. Gopalakrishnan, C. Sürgers, R. Montbrun, A. Singh, M. Uhlarz, and H. v. Löhneysen, *Phys. Rev. B* **77**, 104414 (2008).
- <sup>11</sup>M. Gajdzik, C. Sürgers, M. Kelemen, B. Hillebrands, and H. v. Löhneysen, *Appl. Phys. Lett.* **68**, 3189 (1996).
- <sup>12</sup>S. Kang, G. A. Brewer, J. Battogtokh, R. S. DiPietro, D. Heiman, A. C. Buechele, D. A. McKeown, I. L. Pegg, and J. Philip, *Nanoscience and Nanotechnology Letters* **1**(2), 77 (2009).
- <sup>13</sup>B. D. Cullity, *Elements of X-Ray Diffraction* (Addison Wesley, Massachusetts, 1977).
- <sup>14</sup>J. M. Dubois, G. L. Caera, and J. P. Senateur, *J. Solid State Chem.* **24**, 189 (1978).
- <sup>15</sup>P. Spinat and P. Herpin, *Bull. Soc. Fr. Mineral. Cristallogr.* **99**, 13 (1976).
- <sup>16</sup>G. Colizzi, A. Filippetti, F. Cossu, and V. Fiorentini, *Phys. Rev. B* **78**, 235122 (2008).
- <sup>17</sup>D. P. Kozlenko, I. N. Goncharenko, B. N. Savenko, and V. I. Voronin, *J. Phys.: Condens. Matter* **16**, 6755 (2004).
- <sup>18</sup>K. S. Shankar, K. Sohini, A. K. Raychaudhuri, and G. N. Subbanna, *Appl. Phys. Lett.* **84**, 993 (2004).
- <sup>19</sup>J. J. Neumeier, M. F. Hundley, J. D. Thompson, and R. H. Heffner, *Phys. Rev. B* **52**, R7006 (1995).